*Metallophysics and Advanced Technologies*
*Металофіз. новітні технол.*
*Metallofiz. Noveishie Tekhnol.*
2020, vol. 42, No. 7, pp. 939–948
https://doi.org/10.15407/mfint.42.07.0939
Reprints available directly from the publisher



PACS numbers: 43.25.+y, 68.60.Bs, 71.20.-b, 73.30.+y

# Quantification of Electron Work Function Effects on Acoustic Parameters of Metals

Amel Gacem, Zakaria Hadef*, Kenza Kamli*, and Beddiaf Zaidi**

*University of 20 August 1955, Faculty of Technology, Department of Technology, 26 Road El Hadaiek, 21000 Skikda, Algeria*
**University of 20 August 1955, Faculty of Sciences, Department of Physics, 26 Road El Hadaiek, 21000 Skikda, Algeria*
***University of Batna 1, Faculty of Material Sciences, Department of Physics, Allées 19 Mai, Route de Biskra, 05000 Batna, Algeria*

In this study, efforts are made to establish the correlation between electron work function (EWF) and acoustical properties of metals such as Rayleigh velocity and acoustic impedance. As shown, the generalized Rayleigh velocity increases linearly with increasing EWF. This observed behaviour, which is due to the electronic structures, is also extended and computed for acoustic impedance; exponential dependences are deduced. These dependences are quantified by semi-empirical equations. The obtained results help to better estimate the interdependence between electronic properties of metals and their acoustic parameters.

**Key words:** metals, electron work function, acoustic parameters.

У цьому дослідженні зроблено спробу встановити кореляцію між функцією роботи виходу електрона (EWF) і акустичними властивостями металів, такими як швидкість Релея та акустичний імпеданс. Показано, що узагальнена швидкість Релея лінійно зростає зі збільшенням EWF. Така поведінка, обумовлена електронною структурою, також поширена і обрахована для акустичного імпедансу — було одержано експоненціальні залежності. Ці залежності кількісно описано напівемпіричними рівняннями. Одержані результати допомагають краще оцінити взаємозалежність між електронними властивостями металів та їх акустичними параметрами.

Corresponding authors: Amel Gacem and Zakaria Hadef
E-mails: a.gacem@univ-skikda.dz, z.hadef@univ-skikda.dz or zaki_hd2013@yahoo.fr

Citation: Amel Gacem, Zakaria Hadef, Kenza Kamli, and Beddiaf Zaidi, Quantification of Electron Work Function Effects on Acoustic Parameters of Metals, *Metallofiz. Noveishie Tekhnol.*, **42**, No. 7: 939–948 (2020), DOI: 10.15407/mfint.42.07.0939.

**Ключові слова:** метали, робота виходу електрона, акустичні параметри.

*(Received March 18, 2019)*

## 1. INTRODUCTION

The great use of materials in different fields of technology requires in-depth study of their properties and can lead to deducing relationships between them. For example, the thermodynamic behaviour that governs the interfacial adhesion strength is essentially determined by their elastic [1, 2] and electronic [3] behaviours. Recently, the elastic proprieties are predicted and evaluated by the behaviour of metals electronic work function (EWF). It has been found that Young's modulus of pure metals presents good dependence with their EWFs [4, 5]. The EWF is one of the most important and fundamental parameters of metals, as bulk materials and/or thin films that determine many physical properties of crystal surface [6–10]. It is defined as the energy necessary to extract an electron from a metal Fermi level to infinity or to the vacuum level without kinetic energy. This fundamental propriety plays a major role in various applications involving electron emission from metals, as in photoelectric devices [6]. Various non-destructive techniques are established to characterize the materials properties. Scanning acoustic microscopy (SAM) is one of the important methods for non-destructive determination of elastic properties of metals [11]. This approach, based on the emission and reception of surface acoustic waves (SAWs), is used for the quantitative studies of elastic properties of thin films as well as bulk materials [12]. In this context, a new study has been proposed to determine relationships between work function and acoustic parameters; it shows that these parameters are determined simultaneously *via* acoustic impedances according to the semi-empirical formulas.

## 2. METHODOLOGY AND METALS

### 2.1. Calculation Procedure

In this paper, two approaches are adopted: the first one is the scanning acoustic microscope (SAM) approach [13, 14] and the second one is one parameter (OP) approach [15].

SAM approach consists of theoretical determination of these velocities from the so-called acoustic materials signatures. This analogue signal received by a transducer and focused by the position of the acoustic lens at the sample against the distance $z$, under an incidence angle with the reflected ones [13, 14]; $V(z)$ is the result of the several interferences of all

the leaky wave modes, such as leaky surface acoustic wave, SAW, leaky pseudo-SAW, leaky surface-skimming compressional wave, leaky Lamb wave, and harmonic waves. However, only the velocity of leaky SAW's has been extracted from the $V(z)$ curves in microanalysis mode proposed by Sheppard and Wilson [16] who derived the following expression

$$V(z) = \int_0^{\theta_{\max}} P^2(\theta) R(\theta) [\exp(2jk_0 z \cos\theta)] \sin\theta \cos\theta \, d\theta. \tag{1}$$

Here $P(\theta)$ is the pupil function, $k_0 = 2\pi/\lambda$ is the wave number in the coupling liquid, $j = \sqrt{-1}$, $\theta$ is the half-opening angle of the lens and $R(\theta)$ is the reflection coefficient that is given by

$$R(\theta) = \frac{(Z_{\text{sol}} - Z_{\text{liq}})}{(Z_{\text{sol}} + Z_{\text{liq}})}, \tag{2}$$

where $Z_{\text{sol}}$ and $Z_{\text{liq}}$ are solid and liquid acoustic impedances, respectively; they satisfy the following relationships:

$$Z_{\text{sol}} = \cos^2 2\theta_L + \sin^2 2\theta_T, \tag{3}$$

$$Z_{\text{liq}} = \rho_{\text{liq}} \frac{V_{\text{liq}}}{\cos\theta_{\text{liq}}}, \tag{4}$$

where $Z_{\text{liq}}$ and $Z_{\text{sol}}$ are respectively acoustic impedances of coupling liquid and solid, $V_{\text{liq}}$ is the propagation velocity of the waves in the coupling liquid which has a density $\rho_{\text{liq}}$, $\theta_T$ is the critical angle correspond the excitation of transverse mode. $Z_L$ and $Z_T$ are respectively the longitudinal and transverse acoustic impedances of solid expressed by

$$Z_L = \frac{\rho_{\text{sol}} V_L}{\cos\theta_L}, \tag{5}$$

$$Z_T = \frac{\rho_{\text{sol}} V_T}{\cos\theta_T}. \tag{6}$$

Here $V_L$ and $V_T$ are respectively the longitudinal and transverse velocities of solid which has a density $\rho_{\text{sol}}$ and $\theta_L$ is the critical angle correspond the excitation of longitudinal mode.

The steps of the SAM approach, consist of determining SAW velocities of different modes, calculating acoustic signatures and deducing SAW velocities *via* fast Fourier transform, FFT, treatment of periodic $V(z)$. The details of these steps can be found elsewhere [17, 18].

One parameter approach consists of using the simplified familiar relations of elastic constants into simple relations. Hence, $E$ is expressed in terms of the velocity of just one single mode ($V_L$, $V_T$, $V_R$), as recently reported [15].

$$E = 2.99\rho V_R^2 = 0.575\rho V_L^2 = 2.586\rho V_T^2. \quad (7)$$

The application of these equations removes several limitations related to SAM operational conditions.

### 2.2. Investigated Metals

In this quantification, several isotropic metals are considered with different structural lattices: centred cubic (b.c.c.), face-centred cubic (f.c.c.), and hexagonal compact (h.c.p.). All of them are investigated simultaneously. Different structural characteristics of these metals as well as: the electronic work function, $\varphi$, are taken from [19], Young's modulus values, $E$, are obtained from [20] except (Ag, Au, Pd, Sn) from [21] and densities, $\rho$, are cited from [20]. These characteristics are listed in Table 1. It should be noted that these metals representative of a wide ranges of EWF—2.1 eV < $\varphi$ < 5.3 eV as well as Young's modulus—2 GPa < $E$ < 530 GPa also a wide ranges of densities—1500 kg/m$^3$ < $\rho$ < 22500 kg/m$^3$ and SAW velocities propagation—800 m/s < < $V_R$ < 3100 m/s.

### 2.3. Simulation Conditions

The simulation conditions are those usually used experimentally in the case of a reflexion scanning acoustic microscope, SAM [17, 18]: a half opening angle of the lens of 50°, an operating frequency, $f$ = 150 MHz and Freon as a coupling liquid whose wave velocity, $V_{\text{liq}}$ equal to 716 m/s and density, $\rho_{\text{liq}}$ equal to 1570 kg/m$^3$. The choice of this coupling liquid is imposed by the fact that the majority of studied metals are characterized by slow or medium SAW velocities [21].

## 3. RESULTS AND DISCUSSIONS

### 3.1. Acoustic Signatures Treatment

In OP approach, simplified relations Eq. (6) and some published data of Young's modulus and densities [19, 20] are used to determine SAW velocities; the results are grouped in Table 1. The obtained data of $V_L$ and $V_T$ are then utilized in the SAM approach, *i.e.*, they are used in relations Eq. (1) and Eq. (2) to deduce the $V(z)$ curves of all investigated metals. Typical $V(z)$ results are illustrated in Fig. 1 for some bulk metals: Zr (*a*), Y (*b*), Ce (*c*), and Rb (*d*); it should be noted that similar curves were obtained for all other investigated metals.

It is clear that both curves exhibit oscillatory behaviour due to constructive and destructive interferences between axial beams and the

reflected leaky waves, in the reflection SAM configuration.

The spacing between two successive maxima or successive minima, known as $\Delta z$, differs from different bulk metal.

**TABLE 1.** Characteristics of investigated bulk metals: electronic work function, φ, Young's modulus, $E$, density, ρ, calculated velocities: longitudinal, $V_L$, transversal, $V_T$, and Rayleigh, $V_R$.

| Metal | φ, eV | $E$, GPa | ρ, kg/m$^3$ | OP approach | | | SAM method |
|---|---|---|---|---|---|---|---|
| | | | | $V_L$, m/s | $V_T$, m/s | $V_R$, m/s | $V_{R/\mathrm{SAM}}$, m/s |
| Ag | 4.26 | 83 | 10490 | 5840 | 2806 | 2617 | 2658 |
| Au | 5.10 | 78 | 19300 | 5448 | 2569 | 2389 | 2436 |
| Pd | 5.12 | 117 | 12023 | 6182 | 2915 | 2711 | 2789 |
| Sn | 4.42 | 50 | 6697 | 4332 | 2148 | 2012 | 2100 |
| Rb | 2.16 | 2.35 | 1533 | 1861 | 877 | 816 | 827 |
| Ba | 2.70 | 12.8 | 3512 | 2518 | 1187 | 1104 | 1124 |
| V | 4.30 | 124 | 5960 | 5874 | 2770 | 2576 | 2567 |
| Cr | 4.50 | 248 | 7203 | 6159 | 2904 | 2701 | 2693 |
| Fe | 4.52 | 208 | 7900 | 6191 | 2919 | 2715 | 2704 |
| Nb | 4.30 | 103 | 8570 | 5306 | 2502 | 2327 | 2345 |
| Mo | 4.60 | 329 | 10220 | 6565 | 3096 | 2879 | 2881 |
| Ta | 4.25 | 186 | 16600 | 5129 | 2418 | 2249 | 2245 |
| Ge | 5.00 | 89.6 | 5350 | 5696 | 2686 | 2498 | 2503 |
| Ca | 2.87 | 19.6 | 1540 | 3847 | 1814 | 1687 | 1690 |
| Ni | 5.15 | 207 | 8900 | 6273 | 2958 | 2751 | 2735 |
| Cu | 4.65 | 128 | 8920 | 5612 | 2646 | 2461 | 2454 |
| Rh | 4.98 | 380 | 12440 | 6994 | 3298 | 3067 | 3054 |
| Ir | 5.27 | 527 | 22420 | 6394 | 3015 | 2804 | 2813 |
| Ce | 2.90 | 33.6 | 6670 | 2960 | 1396 | 1298 | 1293 |
| Ti | 4.40 | 116 | 4540 | 5423 | 2557 | 2378 | 2383 |
| Zn | 4.33 | 108 | 7190 | 4935 | 2327 | 2164 | 2176 |
| La | 3.60 | 37 | 6150 | 3710 | 1749 | 1627 | 1618 |
| Hf | 3.90 | 78 | 13312 | 4340 | 2046 | 1903 | 1994 |
| Mg | 3.66 | 44 | 1745 | 4593 | 2166 | 2014 | 2004 |
| Sc | 3.50 | 74.4 | 2989 | 4814 | 2270 | 2111 | 2116 |
| Co | 5.03 | 211 | 8710 | 6330 | 2985 | 2776 | 2785 |
| Y | 3.10 | 63.5 | 4469 | 4308 | 2031 | 1889 | 1880 |
| Zr | 4.05 | 99.3 | 6440 | 5094 | 2402 | 2234 | 2222 |
| Re | 4.96 | 460 | 20530 | 6200 | 2924 | 2719 | 2707 |
| Nd | 3.20 | 41.4 | 7000 | 3207 | 1512 | 1406 | 1404 |
| Gd | 3.10 | 54.8 | 7890 | 3476 | 1639 | 1524 | 1536 |
| Tb | 3.00 | 55.7 | 8270 | 3548 | 1673 | 1556 | 1565 |
| Lu | 3.30 | 68.6 | 9840 | 3601 | 1698 | 1579 | 1587 |

### 3.2. FFT Spectra Analysis

The oscillatory behaviour $\Delta z$ is treated *via* fast Fourier transform, FFT, analysis. The obtained spectra are displayed in Fig. 1. It is well established that under normal operating conditions of the SAM, the most dominating mode is the Rayleigh one. Hence, the principal peak obtained in FFT spectra (Fig. 1) represents such a mode from which the Rayleigh velocity, $V_R$, is deduced according the following formula [13]:

$$V_R = \frac{V_{\text{liq}}}{\sqrt{1 - \left[V_{\text{liq}}/(2f\Delta z)\right]^2}}. \tag{8}$$

The obtained results for Rayleigh velocities of investigated metals are grouped in Table 1. These values are close to those obtained *via* the one parameter approach.

## 4. EFFECTS OF ELECTRONIC WORK FUNCTION

### 4.1. Effects on the Rayleigh Velocity

A theoretical $V_{R-\varphi}$ curve (○○○) is plotted in Fig. 2, collected experimental data of EWF and determined Rayleigh velocities of all investigated metals: (alkali earth metals, transition metals, and rare earth metals). It can clearly be seen that the experimental data of EWF increases with Rayleigh velocity increasing. As shown, these values are

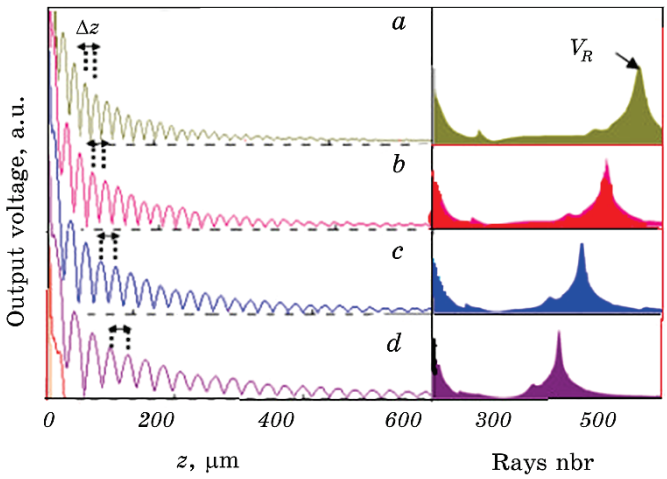


**Fig. 1.** Acoustic signatures and their corresponding FFT spectra for bulk metals: Zr (*a*), Y (*b*), Ce (*c*), and Rb (*d*).

satisfactorily consistent the theoretical curve and thus validate the derived a linear relationship between $V_R$ and φ.

To valorise the validity of obtained results (○○○) in Fig. 2, we plot in the same figure some reported data used one parameter approach for the determination of Rayleigh velocity (▼▼▼) for bulk metals; it is clear that the agreement is quite good.

### 4.2. Quantification of the Results

To quantify the effects of the electron work function on Rayleigh velocity, an optimization method is used to fit all data in Fig. 2. Thus, it is possible to find a linear correlation between $V_R$ and φ for all types of metals:

$$V_R = 629\varphi - 382. \tag{9}$$

The importance of the deuced relation (9) lies in its applicability to all investigated metals. It could be extended, through familiar relations, to other elastic parameters. Similar results for longitudinal and transverse velocities were obtained. Moreover, preliminary results for elastic constants (Young's modulus and shear modulus) are very satisfying.

### 4.3. Effects on the Acoustic Impedances

The acoustic impedance, $Z_{sol}$, is an intensive property of a bulk metal.

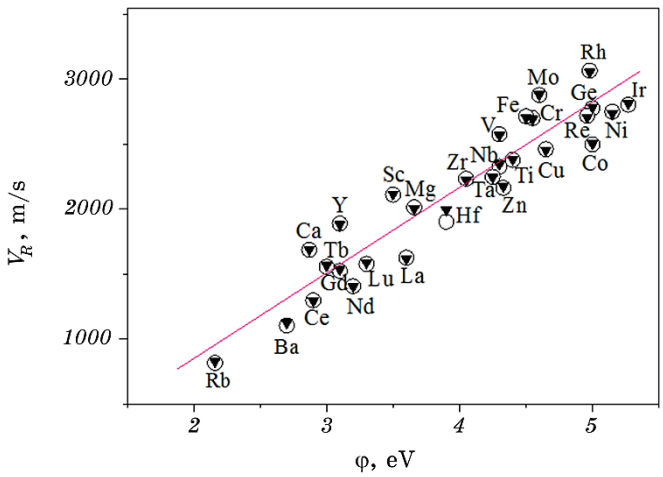


**Fig. 2.** Variations of Rayleigh velocity as a function of the electron work function. Results from SAM method (▼▼▼), from one parameter approach; the line is the best fit.

It characterizes the resistance which opposes the metal to acoustic wave propagation. During this operation, the particles undergo a sinusoidal vibratory displacement around their rest positions. Consequently, their density varies by making regions appear denser and others less dense than when they are at rest. The ratio of these deletions and depressions by the acoustic velocity defines the notion of acoustic impedance [13].

In this context, experimentally obtained values of EWF, yield acoustic impedances of investigated solid metals are determinate by SAM technique to verify the above established $Z_{sol} \sim \varphi$ relationship. Figure 3 illustrates the relation between the yielding acoustic impedances and EWF. As shown, the exponential curve reflects the trend of $Z_{sol} \sim \varphi$ for the solid metal.

It can be observe that the electronic work function increase leads to a non-linear increase of the acoustic impedance. The strongest increase is initially obtained at high values of EWF ($\varphi > 4$ eV). However, for small EWF, the values of $Z_{sol}$ tend towards a pseudo-saturation. To quantify the effects of electronic work function on acoustic impedance an optimization method is used to fit all data presented in Fig. 3. Thus, it is possible to find an exponential correlation between $Z_{sol}$ and $\varphi$ for all types of metals:

$$Z_{sol} = 2 \cdot 10^5 \exp(\varphi). \tag{10}$$

An important point that can be interpreted from the relation (10) is

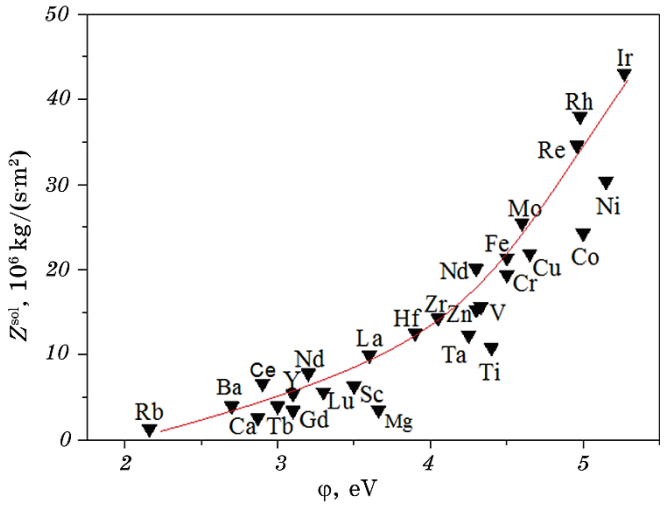


**Fig. 3.** Variations of acoustic impedances as a function of the electronic work function.

the possibility of determining the unknown acoustic impedance of any metal as function of its electronic work function. So, the established relationships help to better understand acoustical properties of metals at an electronic level.

## 5. CONCLUSION

Based on the SAM method and the one parameter approach for determination of acoustic parameters, we have correlated the Rayleigh velocity and acoustic impedance of metals with their EWFs. The dependence of $V_R$ on EWF is quantitatively described by a semi-empirical relation the following linear expression: $V_R = 629\varphi - 382$ for all types of metals. Therefore, it can be concluded that the elasticity or rigidity degree of a metal is very depends on its electronic properties. Moreover, we studied the correlation between $Z_{sol}$ and EWFs of several investigated metals, an exponential behaviour was found and described by $Z_{sol} = 2{\cdot}10^5\exp(\varphi)$. These results are of great importance in the predictions of acoustic and/or elastic behaviour of metals depending on their electronic parameters.

## REFERENCES


1. Z. Hadef, A. Doghmane, and K. Kamli, *Metallofiz. Noveishie Tekhnol.*, **40**, No. 7: 955 (2018).
2. Z. Hadef, *Etude de l'Adhésion dans les Systèmes Métaux Liquides/Céramiques: Micro-Caractérisation Acoustique* (Editions Universitaires Européennes), 978-3-639-50266-4 (2018).
3. J. G. Li, *Mater. Lett.*, **22**, Nos. 3–4: 169 (1995).
4. G. Hua and D. Y. Li, *Appl. Phys. Lett.*, **99**: 041907 (2011).
5. G. M. Hua and D. Y. Li, *phys. status solidi (b)*, **1–4** (2012).
6. J. Chrzanowski and B. Bieg, *Appl. Surf. Sci.*, **461**: 83 (2018).
7. Y. Jiang, J. Li, G. Su, N. Ferri, W. Liu, and A. Tkatchenko, *J. Phys. Condens. Matter*, **29**, 204001 (2017).
8. D. P. Ji, Q. Zhu, and S. Q. Wang, *Surf. Sci.*, **651**: 137 (2016).
9. V. Trepalin, I. Asselberghs, S. Brems, C. Huyghebaert, I. Radu, V. Afanas'ev, M. Houssa, and A. Stesmans, *Thin Solid Films*, **674**: 39 (2019).
10. H. Lu, G. Hua, and D. Li, *Appl. Phys. Lett.*, **103**: 261902 (2013).
11. L. Touati-Tliba, Z. Hadjoub, I. Touati, and A. Doghmane, *Chin. J. Phys.*, **55**: 2614 (2017).
12. Z. Hadef, A. Doghmane, K. Kamli, and Z. Hadjoub, *Prog. Phys. Met.*, **19**, No. 2: 168 (2018).
13. J. Kushibiki and N. Chubachi, *IEEE Trans. Sonics and Ultrasonics*, **32**: 189 (1985).
14. R. G. Maev, *Acoustic Microscopy: Fundamentals and Applications* (Berlin: Wiley-VCH: 2008).
15. M. Doghmane, F. Hadjoub, A. Doghmane, and Z. Hadjoub, *Mater. Lett.*, **61**,

No. 3: 813 (2007).
16. C. G. R. Sheppard and T. Wilson, *Appl. Phys. Lett.*, **38**, No. 11: 884 (1981).
17. P. V. Zinin, *Handbook of Elastic Properties of Solids, Liquids and Gases*, (Eds. M. Levy, H. Bass, R. Stern, and V. Keppens) (New York: Academic Press: 2001).
18. A. Briggs, *Advances in Acoustic Microscopy* (New York: Plenum Press: 1995), vol. 1.
19. H. B. Michaelson, *J. Appl. Phys.*, **48**: 4729 (1977).
20. *ASM Handbook, Pure Metals* (Ohio: ASM International: 1990), vol. 2, ch. 4.
21. G. A. D. Briggs and O. V. Kolosov, *Acoustic Microscopy* (Oxford: Oxford Univ. Press: 2010).